A Symmetry Calibration Procedure for Sensor-to-Airframe Misalignments in Wind Tunnel Data

Dirk Reinhardt, Morten D. Pedersen, Kristoffer Gryte, Tor A. Johansen
Department of Engineering Cybernetics
Norwegian University of Science and Technology
Trondheim, Norway
{dirk.p.reinhardt, morten.d.pedersen, kristoffer.gryte, tor.arne.johansen}@ntnu.no

***Abstract*—We propose a calibration method that transforms data from wind tunnel experiments into a coordinate frame where asymmetries with respect to the symmetry plane of most fixed-wing aircraft are minimized in a least-squares sense. The method applies to all types of aircraft that include a symmetry plane but is particularly relevant for small and low-cost unmanned aerial vehicles (UAVs). Our approach is simple to implement using standard nonlinear program (NLP) solvers. Results for a wind-tunnel data set of a small fixed-wing UAV demonstrate the efficacy of the proposed calibration method.**

***Index Terms*—System Identification, Unmanned Aircraft, Aerodynamic Modeling**

I. Introduction

A. Motivation and Background

Fixed-wing UAV designs are usually symmetric with respect to the longitudinal plane, such that the left-hand side mirrors the right-hand side of the airframe. The goal is for the generalized aerodynamic forces to be symmetric for equivalent maneuvering capabilities during turns in either direction. To identify the forces for a given airframe design, engineers often collect data that capture the forces in wind tunnel tests or flight experiments. In either case, one would expect the magnitude of the forces to be equal for symmetric use of the actuators and mirrored relative velocities concerning the plane of symmetry. However, this is not the case for the collected data when the coordinate axes of the force and moment measurement equipment are not aligned with the coordinate axes of the body-fixed coordinate frame, which is usually the case. This asymmetry then propagates to the identified models and can be problematic in model-based control, which is the use-case we are targeting.

The misalignment can be kept small by careful mounting procedures, such that it is possible to calibrate for remaining asymmetries through proper post-processing. However, it appears that a systematic calibration method to do this has not been addressed, whereas engineering researchers focused on the compensation of other error sources and effects. Molinari et al. [1] consider disturbances due to the airframe and wall of the wind tunnel blocking the airstream. They isolate the airfoil in a pitching motion such that symmetries to sideslip angle variations are not a factor. Damljanovic et al. [2] also focus on wall interference. They note possible offsets between coordinate axes of the measurement equipment and airframe but state that the effects are in the order of magnitude of measurement noise and disregard further calibration. Ocokoljic et al. [3] extensively discuss wind tunnel calibration tests, including the test section, measurement instruments, and standard models for calibration. Jindeog et al. [4] consider possible measurement biases due to thermal effects but only within the longitudinal plane where asymmetries in sideslip angle variations can not be observed. Simmons et al. [5] focus on experiment designs and system identification techniques and do not discuss asymmetries. Holsten et al. [6] notice asymmetries in data series that they expect to be symmetrical but do not offer a solution to compensate for this. The data provided by Ol et al. [7] looks to be sufficiently symmetric, but they do not give detailed information on possible post-processing steps. They note, however, the need for cautious treatment of the actuators. In particular, when testing off-the-shelf radio-controlled UAVs, consumer-grade servos to actuate the control surfaces can introduce significant offsets to the reference deflections due to the hysteresis band. A possible reason for neglecting symmetry considerations in the literature may be that this problem is likely more pervasive for airframes of fixed-wing UAVs that are small and have a low cost.

B. Contribution

This work presents an approach to find a static rotation that aligns the coordinates of the measurement equipment in a wind tunnel experiment with the coordinate axes of the body-fixed frame of a fixed-wing UAV. The necessary assumption that the UAV is symmetric concerning its longitudinal plane is satisfied by most classes of small fixed-wing UAVs and

This work has been carried out at the Center for Autonomous Marine Operations and Systems (NTNU-AMOS) and was supported by the Research Council of Norway through the Centers of Excellence funding scheme, grant no. 223254 - NTNU AMOS, and no. 261791 AutoFly. Corresponding author: Dirk Reinhardt

aircraft. Our approach builds on the formulation of a symmetry condition along the coordinate axes of the force and moment measurement equipment to formulate a suitable error function. We then formulate an optimization problem that finds a transformation that minimizes the asymmetries in the generalized forces (i.e. linear forces and angular momentums) for symmetric relative velocities in a least-squares sense. We base our work on a dataset from a wind tunnel. However, it is straightforward to apply the proposed method to flight data and find the orientation of a relative velocity sensor relative to the body-fixed frame.

C. Organization of the paper

The rest of this paper is structured as follows: section II gives an outline of a dataset obtained in wind tunnel experiments to illustrate the problem of asymmetries. We describe our approach to finding a static transformation that minimizes the asymmetries in the data in section III. Results for the example data are given in section IV before we end with concluding remarks in section V.

II. Problem

Suppose a dataset has been recorded for the purpose of modeling the generalized aerodynamic forces of a fixed-wing UAV. The dataset includes variations of the airspeed, angle of attack, sideslip angle, and control surface deflections. An instructive procedure for obtaining such a dataset is being discussed by Gryte et al. [8], and we will use the resulting data to illustrate the problem of asymmetries. The UAV in the experiments was the Skywalker X8 as depicted in Figure 1 together with its body-fixed coordinate axes $\mathbf{x}^b$, $\mathbf{z}^b \in \mathbb{R}^3$ which span the plane of symmetry.

We start with a description of the data that we use which is from a wind tunnel experiment. However, note that our approach readily generalizes to other test protocols for wind tunnel experiments or flight tests. The only condition is that measurements of the relative velocities are available and that external generalized forces can be observed. This is not a strong limitation for flight tests, considering that inertial measurement units (IMUs) are included in the standard sensor suite.

The collected data is based on the assumption of decoupled dynamics in the lateral and longitudinal plane at small aerodynamic angles. This means that it includes rotations of the lateral plane at zero angles of attack and rotations of the longitudinal plane at zero sideslip angle. The angle of attack was varied between $-10\,\mathrm{deg}$ and $15\,\mathrm{deg}$ with some measurements at higher values and low airspeeds to identify forces in the stall regime. Gryte et al. tested five uniformly spaced elevator deflections between $-20\,\mathrm{deg}$ and $20\,\mathrm{deg}$ at airspeeds set to either $18\,\mathrm{m/s}$ or $21\,\mathrm{m/s}$. With zero aileron deflection and sideslip angle, the data points available for the identification of the longitudinal coefficients are given by

$$(V_a,\, \delta_e,\, \alpha) \in \{18, 21\} \times \{-20, -10, 0, 10, 20\} \times [-10, 15]. \quad (1)$$

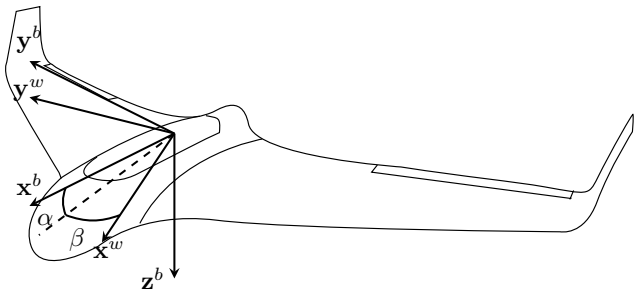

Fig. 1. Drawing of the Skywalker X8 UAV used in the wind-tunnel experiments. The orientation of the wind-frame coordinate axes ($\mathbf{x}^w$, $\mathbf{y}^w$) relative to the body-fixed coordinate axes ($\mathbf{x}^b$, $\mathbf{y}^b$, $\mathbf{z}^b$) defines the angle of attack α and sideslip angle β. The airframe is by design symmetric with respect to the plane spanned by $\mathbf{x}^b$ and $\mathbf{z}^b$.

The dataset for identifying the lateral coefficients includes sideslip angle variations within $-15\,\mathrm{deg}$ and $15\,\mathrm{deg}$ at the same airspeed values as for the longitudinal tests. Based on the assumption of the aileron to be symmetric around zero, the dataset only includes negative deflections. At zero elevator deflection and angle of attack, the lateral data points are given by

$$(V_a,\, \delta_a,\, \beta) \in \{18, 21\} \times \{-20, -10, 0\} \times [-15, 15]. \quad (2)$$

Forces and moments due to the vehicle's weight were compensated during each run. The airframe was carefully mounted onto the force sensor to align the measurement axes with the axes of the body-fixed coordinate frame. The measurement axes are assumed to be in alignment with the axes of the wind tunnel at zero angles of attack and sideslip angles. One would then expect the measurements to be symmetric with respect to zero sideslip angle.

However, the measured dataset does not appear to be symmetric about the longitudinal plane of the airframe, which is shown in Figure 2 for a sweep of sideslip angles. Consider for instance the yaw moment n that is in theory well-approximated by a third-order polynomial of the sideslip angle with zero static component [9]. However, the measurement data depicted in the bottom subplot shows a clear offset at a zero sideslip angle.

We therefore assume a misalignment between the body-fixed coordinate frame that includes the symmetry plane and the measurement frame in which the data is recorded. To formulate the problem, we use elements of the Special Orthogonal Group of order three, denoted by $\mathrm{SO}(3)$. Let the orientation of the body-fixed coordinate frame relative to the measurement coordinate frame be denoted by the symmetric 3×3 rotation matrix $\mathbf{R}_{mb} \in \mathrm{SO}(3)$. The problem is to find the rotation matrix $\mathbf{R}_{mb}$ merely based on the available measurement data that is to be used for model identification and without a prior symmetry calibration routine in the experiments.

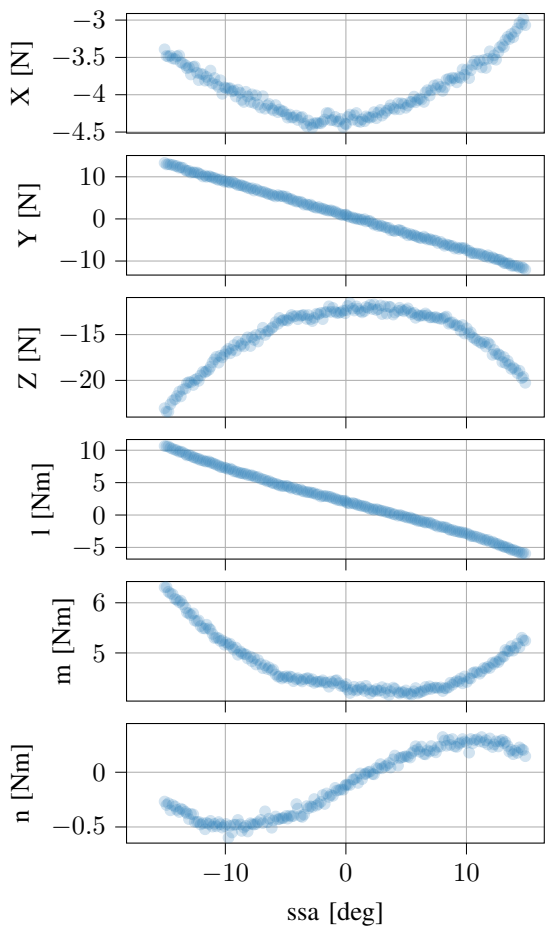

Fig. 2. A sweep of the sideslip angle (ssa) with $\alpha = \delta_a = \delta_e = 0$ and $V_a = 21\text{m/s}$. The measured data does not appear to be symmetric to the longitudinal plane (zero sideslip angle) of the airframe.

III. Method

We begin with a discussion of the symmetry condition and some assumptions on the measurement data. After a brief presentation of the polynomial interpolation of the dataset to generate symmetric measurement pairs and smooth functions that can be used in the NLP, we show how to formulate an optimization problem to find the static transformation to reduce asymmetries in a least-squares sense.

A. Symmetry and Transformations

Let the relative linear velocity $\mathbf{v}_r \in \mathbb{R}^3$ and the relative angular velocity $\boldsymbol{\omega}_r \in \mathbb{R}^3$ be concatenated into one vector $\boldsymbol{\nu}_r = [\boldsymbol{v}_r{}^\top \, \boldsymbol{\omega}_r{}^\top]^\top$. Let the vector of generalized forces be denoted by $\boldsymbol{\tau} = [\mathbf{f}^{b\top} \, \mathbf{m}^{b\top}]^\top$, with force $\mathbf{f}^b \in \mathbb{R}^3$ and momentum $\mathbf{m}^b \in \mathbb{R}^3$ given in the body-fixed frame.

Suppose $\mathbf{f} : \mathbb{R}^6 \mapsto \mathbb{R}^6$ is a mapping from the relative velocities to the generalized forces. The general symmetry condition that we impose is then given by

$$\mathbf{M}\mathbf{f}(\mathbf{M}\boldsymbol{\nu}_r^b) = \mathbf{f}(\boldsymbol{\nu}_r^b). \tag{3}$$

The case of xz-symmetry is defined by the symmetry matrix

$$\mathbf{M} \triangleq \operatorname{diag}(1, -1, 1, -1, 1, -1), \tag{4}$$

which satisfies $\mathbf{M} = \mathbf{M}^{-1} = \mathbf{M}^\top$.

Now suppose that the body-fixed coordinate frame $\{b\}$ and the sensor-fixed frame $\{m\}$ are not aligned, but that the orientation of $\{b\}$ with respect to the coordinate axes of $\{m\}$ is given by a rotation $\mathbf{R}_{mb} \in \mathrm{SO}(3)$. Then we can express the velocity in $\{m\}$ as

$$\boldsymbol{\nu}_r^m = \mathbf{T}\boldsymbol{\nu}_r^b \tag{5}$$

where

$$\mathbf{T} = \begin{bmatrix} \mathbf{R}_{mb} & \mathbf{0} \\ \mathbf{S}(\mathbf{r}_{mb}^m)\mathbf{R}_{mb} & \mathbf{R}_{mb} \end{bmatrix}. \tag{6}$$

The variable $\mathbf{r}_{mb}^m \in \mathbb{R}^3$ denotes the position of the origin of $\{b\}$ with respect to $\{m\}$ in coordinates of $\{m\}$. We make a few simplifying assumptions

***Assumption** 1:* The sensor is placed at the origin of the body-fixed coordinate frame, i.e. $\mathbf{r}_{mb}^m \approx \mathbf{0}$ such that $\mathbf{T} \approx \operatorname{blkdiag}(\mathbf{R}_{mb}, \mathbf{R}_{mb})$ and $\mathbf{T}^{-1} = \mathbf{T}^\top$.
Note that the origin of $\{b\}$ does not necessarily coincide with the center of mass.

***Assumption** 2:* The wind tunnel produces a homogenous air stream with a negligible angular velocity component, i.e. $\boldsymbol{\omega}_r \approx \mathbf{0}$.

Let the coordinate frame of the wind tunnel be described by $\{w\}$. Each data point includes measurements of the relative linear velocity vector in the sensor frame, i.e. $\mathbf{v}_r^m$, typically recorded in terms of airspeed $V_a \in \mathbb{R}$, angle of attack $\alpha \in \mathbb{R}$ and sideslip angle $\beta \in \mathbb{R}$. This can be thought of as magnitude and spherical direction of $\mathbf{v}_r^m$. To parametrize $\mathbf{v}_r^m$ from the data points, we define the map $\boldsymbol{\mu} : \mathbb{R}^3 \mapsto \mathbb{R}^3$ as

$$\mathbf{v}_r^m = \boldsymbol{\mu}(V_a, \alpha, \beta) \triangleq \mathbf{R}_{mw}(\alpha, \beta)\begin{bmatrix} V_a & 0 & 0 \end{bmatrix}^\top \tag{7}$$

and its inverse

$$\begin{aligned}(V_a, \alpha, \beta) &= \boldsymbol{\mu}^{-1}(\mathbf{v}_r^m) \\ &\triangleq \left(\|\mathbf{v}_r^m\|_2, \arctan\left(\frac{w_r}{u_r}\right), \arcsin\left(\frac{v_r}{\|\mathbf{v}_r^m\|_2}\right)\right),\end{aligned} \tag{8}$$

where $\mathbf{v}_r^m = \begin{bmatrix} u_r & v_r & w_r \end{bmatrix}^\top$. The rotation matrix $\mathbf{R}_{mw}(\alpha, \beta) = \mathbf{R}_{ms}(\alpha)\mathbf{R}_{sw}(\beta)$ is a composition of

$$\mathbf{R}_{ms}(\alpha) = \begin{bmatrix} \cos(\alpha) & 0 & \sin(\alpha) \\ 0 & 1 & 0 \\ -\sin(\alpha) & 0 & \cos(\alpha) \end{bmatrix} \tag{9}$$

and

$$\mathbf{R}_{sw}(\beta) = \begin{bmatrix} \cos(\beta) & \sin(\beta) & 0 \\ -\sin(\beta) & \cos(\beta) & 0 \\ 0 & 0 & 1 \end{bmatrix}, \tag{10}$$

which are the known rotation matrices between body-fixed frame, stability frame and wind frame [10].

B. Interpolating the dataset

Our goal is to formulate an optimization problem to find the rotation matrix $\mathbf{R}_{mb}$ based on the available force measurements in the dataset from which expressions for both sides of (3) can be derived. To be able to use gradient-based optimization methods, we need to approximate the measurements by functions that are continuously differentiable with respect to the sideslip angle. In this subsection we give an outline how this can be done using polynomial interpolation. For each sweep of sideslip angles, the airspeed V_a, the angle of attack α and elevator deflection δ_e are constant. Moreover, we only consider sweeps during which the aileron deflection δ_a is set to zero, given that a non-zero value would violate the symmetry condition. The aileron deflections are assumed to be offset-free. This assumption is hard to satisfy in practice when consumer-grade servo motors to actuate the control surfaces are used.

To interpolate between data points and to provide smooth functions to the optimizer, we fit polynomial functions of the sideslip angle to the recorded aerodynamic coefficients. The functions are defined as

$$f_{C_k}(\beta) = \sum_{i=0}^{n} a_i \beta^i. \tag{11}$$

Given the measurements $(C_X, C_Y, C_Z, C_l, C_m, C_n)$, the coefficients a_i in the functions f_{C_k} can be found by using linear regression for each sweep of the sideslip angle. Upon inspection of the measured aerodynamic coefficients with varying sideslip angle, we found a good compromise between a reasonable fit and low polynomial order $n = 4$ for C_D, C_L, C_m, $n = 3$ for C_l, C_n and $n = 1$ for C_Y.

We then concatenate the functions f_{C_k} to approximate the function $\mathbf{f}$ in (3) by $\hat{\mathbf{f}}$ defined as

$$\hat{\mathbf{f}}(\boldsymbol{\nu}_r^m | \delta_a, \delta_e) \triangleq \begin{bmatrix} f_{C_x}(\beta) \\ f_{C_Y}(\beta) \\ f_{C_Z}(\beta) \\ b f_{C_l}(\beta) \\ c f_{C_m}(\beta) \\ b f_{C_n}(\beta) \end{bmatrix}, \tag{12}$$

where $b, c \in \mathbb{R}_{\geq 0}$ denote wingspan and chord length of the airframe, respectively. Note that angle of attack and control surface deflections are implicit in the polynomials f_{C_k}. In addition to the angle of attack, the airspeed and sideslip angle can be obtained by the map $\boldsymbol{\mu}^{-1}$.

To obtain the reflected relative velocity vector in $\{m\}$, the measured relative velocity vector first needs to be transformed to $\{b\}$ using (5), then reflected using (4), and transformed back to $\{m\}$ again. This leads to the reflected relative velocity vector $\boldsymbol{\nu}_r'^m$ given as

$$\boldsymbol{\nu}_r'^m = \mathbf{T}\mathbf{M}\mathbf{T}^{-1}\boldsymbol{\nu}_r^m, \tag{13}$$

in which the expression $\mathbf{T}\mathbf{M}\mathbf{T}^{-1}$ can be interpreted as a similarity transformation of the reflection matrix $\mathbf{M}$ to the measurement frame $\{m\}$.

C. Optimization problem

The symmetry condition (3) can be used to formulate an error $\mathbf{e} \in \mathbb{R}^6$ in the body-fixed frame based on the interpolation polynomials as

$$\mathbf{e} = \mathbf{M}\mathbf{T}^{-1}\hat{\mathbf{f}}(\mathbf{T}\mathbf{M}\mathbf{T}^{-1}\boldsymbol{\nu}_r^m | 0, \delta_e) - \mathbf{T}^{-1}\hat{\mathbf{f}}(\boldsymbol{\nu}_r^m | 0, \delta_e). \tag{14}$$

We use $\mathbf{e}$ to formulate a cost function as the sum over all sideslip angle sweeps with zero aileron deflection. Let the set of all suitable sweeps be denoted by $\mathcal{D}$ and the samples in each sweep be denoted by $N_{\mathcal{D}}$, then the cost function is defined as

$$J = \sum_{\mathcal{D}} \sum_{i}^{N_{\mathcal{D}}} \mathbf{e}_i{}^{\top} \mathbf{e}_i. \tag{15}$$

Suppose the matrix $\mathbf{R}_{mb}$ is parametrized by at set of Euler angles. Then it can be shown that the similarity transformation $\mathbf{T}\mathbf{M}\mathbf{T}^{-1}$ is invariant to rotations around a vector that is normal to the xz-plane, i.e. pitch rotations. This means that it is enough to use roll angle $\phi \in [\underline{\phi}, \overline{\phi}]$ and yaw angle $\psi \in [\underline{\psi}, \overline{\psi}]$, where $\underline{\cdot}, \overline{\cdot}$ denote a respective lower and upper bound. The parametrization of $\mathbf{R}_{mb}$ is

$$\mathbf{R}_{mb}(\phi, \psi) = \begin{bmatrix} \cos(\psi) & \sin(\psi) & 0 \\ -\cos(\phi)\sin(\psi) & \cos(\phi)\cos(\psi) & \sin(\phi) \\ \sin(\phi)\sin(\psi) & -\sin(\phi)\cos(\psi) & \cos(\phi) \end{bmatrix}. \tag{16}$$

We then find the optimal values ϕ^*, ψ^* by solving the NLP

$$\phi^*, \psi^* \triangleq \arg\min_{\phi,\psi} J(\phi, \psi) \tag{17}$$

$$\text{s.t.} \quad \underline{\phi} \leq \phi \leq \overline{\phi} \tag{18}$$

$$\underline{\psi} \leq \psi \leq \overline{\psi} \tag{19}$$

and denote the resulting rotation matrix as $\mathbf{R}_{mb}^*$ and the transformation as $\mathbf{T}^*$.

Remark 1: The outlined problem of finding a static rotation matrix to minimize the cost function (15) is similar to Wahba's problem [11] if Assumption 1 is satisfied. If one can show equivalence of the cost function given here to the loss function used in [11], it is possible to use Davenport's q-method [12] to arrive at an explicit solution to the optimization problem.

IV. Results

We use algorithmic differentiation provided by CasAdi [13] and the interior-point optimization implemented in interior point optimizer (Ipopt) [14] to solve the optimization problem defined by (17) - (19).

For the given wind-tunnel data set, the optimal solution to the calibration problem is given by $\phi^* = -0.90\,\text{deg}$ and $\psi^* = 1.58\,\text{deg}$, which is in the range that can not be corrected for via visual inspection by the operator conducting the wind tunnel experiment. The result for a sweep of the sideslip angle during which $\alpha = \delta_a = \delta_e = 0$ and $V_a = 21\,\text{m/s}$ is depicted in Figure 3. Clearly, the measured forces and moments do not look symmetric with respect to the longitudinal plane, i.e. when $\beta = 0$. However, when plotted

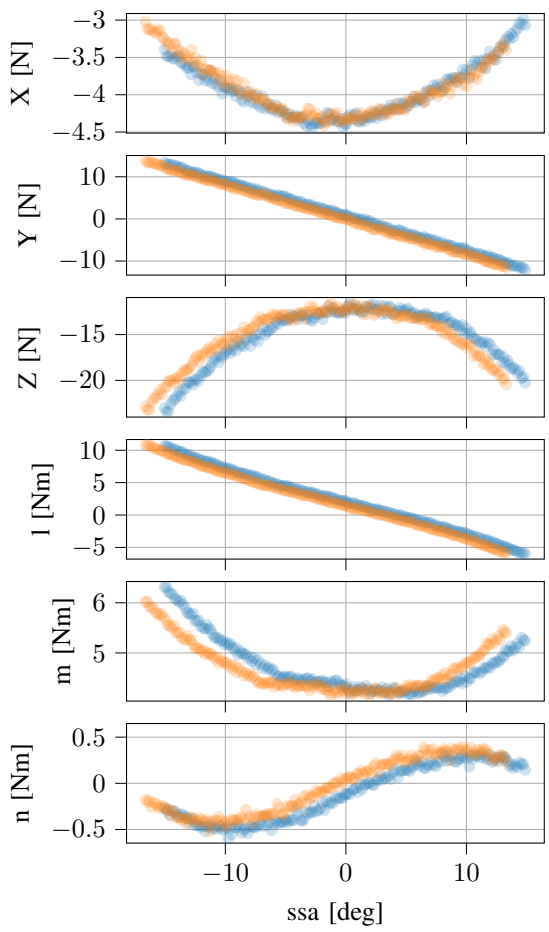

Fig. 3. A sweep of the sideslip angle (ssa) with $\alpha = \delta_a = \delta_e = 0$ and $V_a = 21\mathrm{m/s}$. The data over the measured sideslip angle (blue) and the data over the calibrated sideslip angle (orange) are plotted. The calibration angles are $\phi^* = -0.90\,\mathrm{deg}$ and $\psi^* = 1.58\,\mathrm{deg}$.

over the calibrated sideslip angle, most of the forces and moments look symmetric. The exception is the roll moment l. A possible cause for this can be that the airframe that was used in the experiments has asymmetries with respect to the xz-plane. Another explanation is that the wind tunnel may be producing a vortex around its longitudinal axis that would produce a non-zero relative angular velocity and therefore violate Assumption 2. In the latter case, the calibration could be extended to estimating the relative angular velocity

$$\boldsymbol{\omega}_r^w = \begin{bmatrix} p_r & 0 & 0 \end{bmatrix}^\top, \tag{20}$$

with $p_r \in \mathbb{R}$ as an additional decision variable in the optimization.

Yet another possibility is that the control surface deflections were not symmetric and therefore inducing an additional roll moment. The identification of the aerodynamic model is out of scope of this work, but we discuss it in a separate paper [15]. The resulting aerodynamic model of the roll moment shows that an aileron deflection of less than $2.5\,\mathrm{deg}$ is enough to explain the offset of approximately $2\,\mathrm{N\,m}$ in Figure 3. Mapped to the elevon deflection, this amounts to $1.25\,\mathrm{deg}$ on each side, which is within the hysteresis band for the consumer-grade servos that were used during the tests. It is advised to use more advanced servos that send position feedback to compensate for this effect and have more information in the dataset in general.

V. Conclusion

We presented a method to reduce planar asymmetries in a dataset obtained in wind tunnel tests with a fixed-wing UAV that is by design symmetrical. The optimization procedure that finds the rotation of the body-fixed coordinate frame to the measurement equipment is simple to implement with standard NLP solvers. Calibration of a dataset of a small fixed-wing UAV demonstrated the efficacy of this approach, and we concluded with a discussion on other possible sources of asymmetries. Future work should consider servo motors that actuate the control surfaces with higher accuracy and position feedback to eliminate other sources of asymmetries.

References

[1] G. Molinari, A. F. Arrieta, M. Guillaume, and P. Ermanni, "Aerostructural performance of distributed compliance morphing wings: Wind tunnel and flight testing," *AIAA Journal*, vol. 54, no. 12, pp. 3859–3871, 2016. [Online]. Available: https://doi.org/10.2514/1.J055073

[2] D. Damljanović, J. Isaković, and B. Rašuo, "T-38 wind-tunnel data quality assurance based on testing of a standard model," *Journal of Aircraft*, vol. 50, no. 4, pp. 1141–1149, 2013. [Online]. Available: https://doi.org/10.2514/1.C032081

[3] G. Ocokoljic, D. Damljanovic, D. Vukovic, and B. Rašuo, "Contemporary frame of measurement and assessment of wind-tunnel flow quality in a low-speed facility," *FME Transactions*, vol. 46, no. 4, pp. 429–442, 2018.

[4] C. Jindeog, L. Jangyeon, S. Bongzoo, and K. Samok, "Wind tunnel test of an unmanned aerial vehicle (uav)," *KSME international journal*, vol. 17, no. 5, pp. 776–783, 2003.

[5] B. M. Simmons, H. G. McClelland, and C. A. Woolsey, "Nonlinear model identification methodology for small, fixed-wing, unmanned aircraft," *Journal of Aircraft*, vol. 56, no. 3, pp. 1056–1067, 2019. [Online]. Available: https://doi.org/10.2514/1.C035160

[6] J. Holsten, T. Ostermann, and D. Moormann, "Design and wind tunnel tests of a tiltwing uav," *CEAS Aeronautical Journal*, vol. 2, no. 1, pp. 69–79, Dec 2011. [Online]. Available: https://doi.org/10.1007/s13272-011-0026-4

[7] M. Ol, C. Zeune, T. White, and T. Kudla, "Wind tunnel evaluation of powered static aerodynamics of an aerobatic uav," in *51st AIAA Aerospace Sciences Meeting including the New Horizons Forum and Aerospace Exposition*, 2013. [Online]. Available: https://arc.aiaa.org/doi/abs/10.2514/6.2013-241

[8] K. Gryte, R. Hann, M. Alam, J. Rohác, T. A. Johansen, and T. I. Fossen, "Aerodynamic modeling of the Skywalker X8 Fixed-Wing Unmanned Aerial Vehicle," *International Conference of Unmanned Aerial Systems*, 2018.

[9] J. A. Grauer and E. A. Morelli, "Generic global aerodynamic model for aircraft," *Journal of Aircraft*, vol. 52, no. 1, pp. 13–20, 2015. [Online]. Available: https://doi.org/10.2514/1.C032888

[10] R. W. Beard and T. W. McLain, *Small unmanned aircraft: Theory and practice*. Princeton University Press, 2012.

[11] G. Wahba, "A least squares estimate of satellite attitude," *SIAM Review*, vol. 7, no. 3, pp. 409–409, 1965. [Online]. Available: https://doi.org/10.1137/1007077

[12] F. L. Markley and J. L. Crassidis, *Fundamentals of Spacecraft Attitude Determination and Control*. Springer-Verlag New York, 2014.

[13] J. A. E. Andersson, J. Gillis, G. Horn, J. B. Rawlings, and M. Diehl, "CasADi – A software framework for nonlinear optimization and optimal control," *Mathematical Programming Computation*, In Press, 2018.

[14] A. Wächter and L. T. Biegler, "On the Implementation of a Primal-Dual Interior Point Filter Line Search Algorithm for Large-Scale Nonlinear Programming," *Mathematical Programming*, vol. 106, no. 1, pp. 25–57, 2006.

[15] D. Reinhardt, K. Gryte, and T. A. Johansen, "Modeling of the Skywalker X8 Fixed-Wing UAV: Flight Tests and System Identification," in *2022 International Conference on Unmanned Aircraft Systems (ICUAS)*, submitted.